The impact of anion elements on the engineering of the electronic and optical characteristics of the two dimensional monolayer janus MoSSe for nanoelectronic device applications

Barakat, Fatimah; Laref, Amal; AlSalhi, Mohamad ; Faraji, Shirin

Published in:
Results in Physics

DOI:
10.1016/j.rinp.2020.103284

Publication date:
2020

Results in Physics 18 (2020) 103284

Contents lists available at ScienceDirect

Results in Physics

journal homepage: www.elsevier.com/locate/rinp

The impact of anion elements on the engineering of the electronic and optical characteristics of the two dimensional monolayer janus MoSSe for nanoelectronic device applications

F. Barakat[a], A. Laref[a,*], Mohamad S AlSalhi[a], S. Faraji[b]

[a] Physics department, Faculty of Science, King Saud University, Riyadh, Saudi Arabia
[b] Zernike Institute for Advanced Materials, University of Groningen, The Netherlands

ARTICLE INFO

Keywords:
Doping janus MoSSe monolayer
2D material properties
Optical spectra
Nanocomposites
Electronic devices

ABSTRACT

Two-dimensional (2D) materials have gained prominent attention in the nano-electronics arena, owing to their tunable electronic and optical features. Here, the physical properties of a janus MoSSe monolayer are examined upon the chemically co-doping of S/Se sites by non-metallic and halogen elements (C, Si, N, P, As, and F) employing first-principles calculations. Accordingly, an alteration of both the upper valence and the lower conduction states is revealed for janus MoSSe monolayer upon the replacement of both S and Se anion host atoms by sp-elements (C, Si, N, P, As, and F). A shift in the lowest conduction band underneath the Fermi energy level (E_F) occurs in janus MoSSe monolayer when both S and Se elements are replaced by (F, F) atoms. This effectively conducted to a system with an n-type character. In contrast, the highest valence bands moved upward E_F owing to the co-doping effect of C, Si, N, P, and As atoms on the janus MoSSe monolayer with p-type nature. The key features of the optical spectra, such as the optical absorption, reflectivity, and electron loss functions of the co-doped janus MoSSe monolayer are inspected. Our results imply a modification in the low-energy photon regime of the co-doped janus MoSSe monolayer at S and Se host atoms by non-metallic sp-elements comparatively to the free-standing monolayer. A reduction in the optical absorption and an increase in the reflectivity at low-energy photon window are detected when the janus MoSSe monolayer is co-doped by (C, Si), (N, P), (P,As), and (F,F) elements, respectively at S and Se chalcogen atoms. The current study infers that the co-doping S and Se sites of janus MoSSe monolayers, with sp- elements, can be beneficial in the future applications of 2D materials for the field-effect transistors and nano-electronic devices.

Introduction

Two-dimensional (2D) materials grant a novel avenue for studying the underlying physics beyond the limit of their bulk systems, and they have acquired various technological applications. The exploration of 2D monolayer materials represent an interesting topic after the successful fabrication of a 2D monolayer graphene, which was reported in 2004 [1]. The striking features of the first 2D material discovered, i.e., graphene, exhibited peculiar thermal, mechanical, and electrical behaviours [2], whereas the absence of a sizable energy gap restricts its functionalities in logic devices. For this main reason, researchers were looking for systems analogous to graphene with better electronic performance and they have explored a variety of 2D materials, such as transition metal dichalcogenide (TMDC) MoS_2 [3], hexagonal boron nitride (h-BN), and black phosphorus (BP) [4]. These 2D materials have been broadly scrutinized owing to their interesting features, specifically their few-atomic or mono-atomic layer thickness. Like graphene, TMDCs represent a category of layered materials that illustrate a band gap, and their bonding character is strong in-plane [5]. In view of this, the typical 2D-TMDC, i.e., the molybdenum disulphide (MoS_2) monolayer, which is an adaptable material with versatile functionalities, has been investigated because of its prominent usage in photoluminescence [6], lithium ion batteries (LIBs) [7], photodetectors [8], flexible electronic devices [9], and field effect transistors [10,11].

Various experimental works have developed technological paradigm of MoS_2 monolayer-based piezoelectric nanogenerators, which can be applied to the field of energy harvesting [12,13]. In addition, 2D materials, such as MoS_2 systems are also applied in triboelectric devices to produce a larger electricity harvest [14] and an unceasing direct current [15] owing to their flat surface and wide contact surface. Layered materials are predominantly touted as the next-generation systems to scale different electronic and information technology devices

* Corresponding author.
E-mail addresses: fbarakat@KSU.EDU.SA (F. Barakat), alaref@ksu.edu.sa (A. Laref), malsalhi@KSU.EDU.SA (M.S. AlSalhi), s.s.faraji@rug.nl (S. Faraji).

https://doi.org/10.1016/j.rinp.2020.103284
Received 23 June 2020; Received in revised form 27 July 2020; Accepted 28 July 2020
Available online 02 August 2020

[16]. Therefore, the preparation of a MoS_2 monolayer is established by mechanical and liquid exfoliation [17,18]. Interestingly, the implementation of exfoliated TMDCs is realized in light-emitting diodes, thin-film transistors, and photodiodes [19–21]. In the recent years, the 2D materials have been developed with superior quality, by employing the chemical vapour deposition (CVD) process to illustrate the possible wide-scale fabrication of these materials [22]. More significantly, TMDCs possess an additional range of characteristics, comparatively to graphene. These can be used to mass-produce heterogeneous 2D devices with peculiar features [23]. Hence, the focus of study relies on the alteration of the structural and engineering functional of 2D materials, to determine their novel properties [24–40].

Very recently, the synthesis of janus transition-metal dichalcogenide MoSSe monolayer has been characterized [30]. In the synthesis, a strategy has been developed for breaking the symmetry of out-of-structural plane to produce a new structural phase, the so-called janus MoSSe monolayer. The authors exhibited that the replacement of the upper layer of Se atoms by S atoms and the sulphurisation could be controlled in the $MoSe_2$ monolayer [30]. The successful synthesis of the janus MoSSe monolayer in the hexagonal (2H) phase has been performed through the initial MoS_2 monolayers by utilizing the CVD and thermal selenisation techniques with a complete substitution of the upper layer of S atoms with Se atoms [30]. This eventually results in a structural crystalline configuration by sandwiching Mo atom layer between S, and Se layers. The ultimate bulk structure was found to have a semiconducting character with an indirect band gap of 1.5 eV. These janus monolayer materials can be useful for nanoscale energy conversion device applications. Previous researches reported that the replacement of Mo by other transition metals can affect the alteration of semiconductor characteristics of the monolayer to a magnetic state [26–30]. This structural variation is expected to develop various beneficial modification in the optical and electronic features of the monolayer. Currently, an optical gap of 1.8 eV has been reported, which is close to the average optical gaps of MoS_2 and $MoSe_2$ [31].

It is well recognized that the substitution in 2D materials or the vacancy defects therein are fruitful for tuning their physical characteristics. For instance, the tailoring of magnetic states in graphene and boron nitride were established by creating vacancies [32,33]. Unlike those in graphene and boron nitride, some typical vacancies can be detected in MoS_2 monolayer by using CVD. These involve mono-sulphur vacancy (VS), di-sulphur vacancy (VS_2), and rows created by several sulphur vacancies [34,35]. Therefore, it is not revealed whether a vacancy or a substitution can induce a modification of the physical characteristics of janus MoSSe monolayer. Co-doping of the host lattice is a practical technique to tune or improve the physical behaviours, such as the electrical and optical characteristics, of this monolayer. Similarly, alloying MoS_2 and $MoSe_2$ can produce beneficial properties, which are absent in binary bulks [36–39]. However, the physical behaviors of janus MoSSe monolayer co-doped with sp- anion elements have not been reported yet. Thus, we conducted a systematic study regarding the co-doping of janus 2H-MoSSe monolayer by substituting the anion elements at S and Se sites. The electronic and optical features of the co-doping effects of sp-elements (C, Si, N, P, As, and F atoms) on janus 2H-MoSSe monolayer with a 3 × 3 supercell have not been investigated so far. Our investigation will provide useful information for performing future experimental works on this promising 2D material. From our results, we found that the co-doping of (S,Se) host atoms by (F,F) elements had the lowest formation energy, indicating the stable structure among the remaining co-doped systems. The other co-doping elements had higher formation energies than the doping of (F, F) atoms instead of (S,Se) host sites of the janus 2H-MoSSe monolayer having a 3 × 3 supercell. These various co-doping elements can alter the electronic band structures of the janus MoSSe monolayer.

The aim of this work is to systematically examine the evolution of the electronic band structures and optical behaviours of the pristine janus 2H-MoSSe monolayer with a 3 × 3 supercell and its counterpart co-doping of (S,Se) host atoms by sp- non-metallic elements (C, Si, N, P, As, and F atoms) to acquire a p-type or an n-type character. In this respect, we investigate the substitutional impact of C, Si, N, P, As, and F atoms on the electronic and optical properties of freestanding janus 2H-MoSSe monolayer. It is worth noting that the 2sp non-metallic elements (N and F) are positioned in the same row as C element, the other 3sp-element (P) is located in the same row as Si element of the subgroup of S atom, and the last 4sp element (As) belongs to the subgroup of Se atom. For this main reason, we perform a theoretical investigation to analyze the various physical properties of the undertaken systems using density functional theory (DFT) [41] within the framework of a pseudopotential scheme, as portrayed by Vienna Ab initio Simulation Package (VASP) [42–44]. Moreover, for the exchange–correlation functional, the generalized gradient approximation (GGA) is employed [41]. It is revealed that the bonding character can change from the pure to p-type or n-type of janus 2H-MoSSe monolayer. Importantly, the positions and intensity optical spectra of the pure and p-type as well as n-type of 2H-MoSSe monolayer are altered. This can conduct to the tremendous potential functionalities in the nanoelectronic devices based on 2H-MoSSe monolayer. Furthermore, it is indicated that the doping impact on 2H-MoSSe monolayer modifies its electronic structures and optical properties from the visible to the infrared (IR) regime. Thereafter, the current investigation offers an elucidation into the tailoring of 2D electronic structures, besides to the optical properties of these 2D materials that could be beneficial for optoelectronic device applications.

The organization of the paper is classified as follows. In Section 2, a concise representation of the computational calculations is provided. The results and discussion are analyzed in Section 3. Finally, the main points of our results are concluded in Section 4.

Computational calculations

By employing the DFT based on pseudopotential method, we have carried out our calculations, as described by VASP code [42]. This method is founded on a plane-wave basis set. The interaction between ion cores and valence electrons is represented by projector augmented wave (PAW) potentials [43]. The addition of the nonlocal corrections is provided in the form of the GGA scheme within Perdew-Burke-Ernzerhof (PBE) exchange and correlation functionals [41]. The plane-wave basis set holds an energy cut-off up to 450 eV, and an augmentation charge cut-off of 650 eV was utilized for ensuring a good convergence of the total energies. A geometric relaxation was established with a conjugate gradient minimization scheme. The estimation of the error bar of the absolute energies was determined in the overall calculations to be approximately 2 meV/atom by converging the tests of the energy cut-off and k-point sampling. In our case, we considered a free-standing janus MoSSe monolayer within a 3 × 3 unit cell and a vacuum of 18 Å to prevent significant slab interactions. A 17 × 17 × 1 k-mesh created by the Monkhorst-Pack method [45] is utilized. All the atomic positions were relaxed in the plane, and the vertical positions were kept fixed. Gaussian smearing was performed about 0.1 eV to facilitate a prompt convergence of the co-doping of the janus 2H-MoSSe monolayer with a 3 × 3 supercell by substituting S and Se atomic sites with the sp- elements (C, Si, N, P, As, and F). As portrayed in Fig. 1, the creation of the structure was built-up by the substitution of one S atom layer of the MoS_2 monolayer with a Se layer. The resulting structure has a Mo atom layer sandwiched between the S and the Se atomic layers. The equilibrium lattice parameters a_0 and c_0 for the janus 2H-MoSSe monolayer are computed to be around 3.23 Å and 13.8 Å, respectively, which are in accordance with the previous experimental works [25,29–31]. The 2D schematic representation of the janus MoSSe monolayer displays the top view of the MoSSe structure, with the chalcogen atoms S and Se in yellow and green, respectively, and the metal atoms (Mo) in purple (Fig. 1). The configurations of the relaxed janus 2H-MoSSe monolayer with a 3 × 3 supercell for both

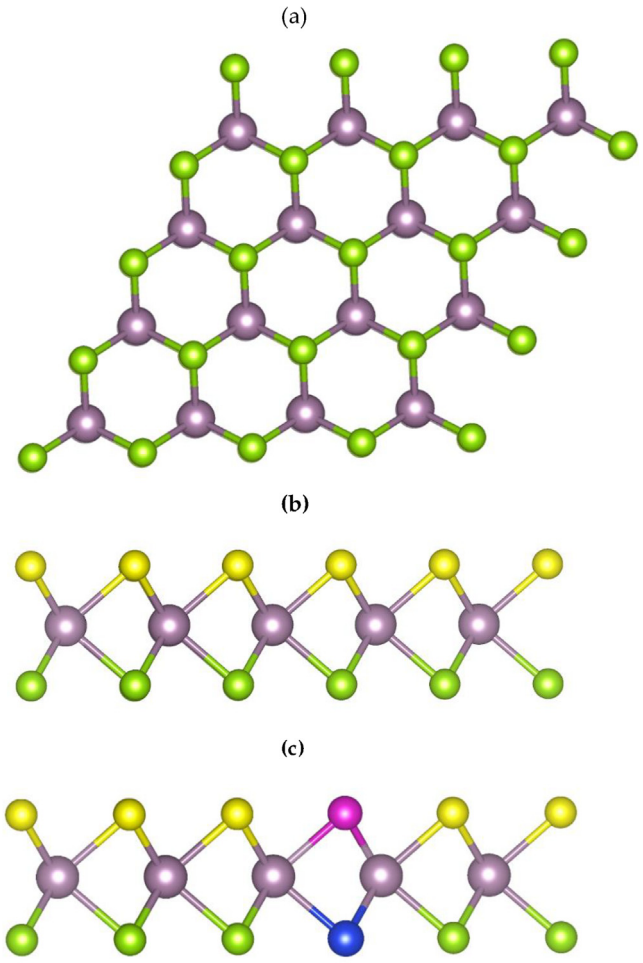

Fig. 1. The (a) top-view and (b) side view of the structural geometries used in our calculations of pure 2H-MoSSe-3x3 supercell structure having janus monolayer (Mo atom (purple), yellow atom S (yellow), and the Se atom (green)). One sulfur atom is substituted by C, N, P, and F elements, respectively, in the upper part of layer and selenium atom is substituted with Si, P, As, and F atoms in the lower part of layer of MoSSe janus-monolayers (MoSSe-CSi, MoSSe-NP, MoSSe-NAs, MoSSe-PAs, and $MoSSeF_2$), as indicated in lower panel (c). The structural lattice parameters are a = 3.23 Å; and c = 13.8 Å (a) Top view of the pristine 3x3 supercell MoSSe janus monolayer, (b) the side view of MoSSe janus-monolayer. For both upper and lower parts of layers, the coordination of each of the Mo atoms with 3 S and 3 Se atoms is represented in a triangular prismatic fashion. (For interpretation of the references to colour in this figure legend, the reader is referred to the web version of this article.)

pristine and co-doped MoSSe monolayer sheets are depicted in Fig. 1. They are produced by replacing one S atom with C, N, P, and F elements, respectively, in the upper layer and one Se atom by Si, P, As, and F atoms, respectively, in the lower layer of the monolayer (MoSSe-CSi, MoSSe-NP, MoSSe-NAs, MoSSe-PAs, and $MoSSeF_2$). The calculated electronic and optical characteristics of the freestanding and co-doped janus 2H-MoSSe monolayer sheets with a 3 × 3 supercell are discussed in the subsequent sections and are established with HSE06 scheme.

Results and discussions

Structural properties of the janus MoSSe monolayer and its counterpart co-doped with non-metallic elements (C, Si, N, P, As, and F atoms)

The structural geometries are first optimised for the pure janus 2H-MoSSe monolayer at the equilibrium lattice constants of the hexagonal structure: a_0 = 3.23 Å and c_0 = 13.8 Å, which are obtained after performing the total energy minimization vs. the structural cell parameters. The structure is particularly acquired by the lattice parameters *a* and *c* (the lattice parameters of hexagonal structure). The lattice parameters agree fairly well with the previous experimental results of 4% [37]. In the MoSSe monolayer, the Mo atom shares a covalent bonding with three S atoms in the upper plane and to three Se atoms in the lower plane. They constitute a trigonal prism structure, which is joined to six in-plane Mo atoms in an hexagona pattern like-graphene. In contrast, each S or Se atom is bonded to three out-of-plane Mo atoms and is connected to six in-plane S or Se atoms with a hexagonal arrangement. The Mo-S and Mo-Se bonding distances are equal to 2.38 Å and 2.46 Å, respectively (see Fig. 1). The basis cell of a janus MoSSe monolayer is composed of three atoms (i.e., Mo, S, and Se), having a repetition on each atomic site of a 2D hexagonal lattice. (Fig. 1).

The formation energy provides a straightforward information about the stability and the feasible growth process of complex 2D materials. Note that the lower formation energy can conduct to the favourable tendency of formation of complex 2D material. $E_{Formation}$ is computed from the difference of the total energy of crystal and summation of energy of the corresponding stable components. The computed formation energies are carried out within GGA technique. The formation energy of a specific substitutional codopant, E_{form}, is denoted by:

$$E_{Formation} = E_{Total}\,(MoSSe + A + B) + E_{bulk}(host) - E_{Total}\,(MoSSe) - E_{bulk}(A) - E_{bulk}(B)$$

Here, $E_{Total}\,(MoSSe + A + B)$ indicates the total energy of the system that inserts the substitutional atoms (A, B) in place of (S, Se) host chalcogen atoms of the janus MoSSe monolayer. One atom S is substituted by one atom A in the upper part layer and one substitutional atom B instead of one atom Se in the lower layer part of the janus MoSSe sheet. (A,B) = (C, Si), (N, P), (P, As), (N, As) and (F, F), respectively are the substitute of (S, Se) anion atoms in both the upper and lower layers. $E_{Total}\,(MoSSe)$ represents the total energy of the pristine MoSSe janus monolayer. Note that $E_{bulk}(host)$ denotes the energy of substituted S (Se) host chalcogen atom in bulk form, while $E_{bulk}(A)$, and $E_{bulk}(B)$ indicate respectively the energies of the substitutional atoms (C, Si, N, P, As, and F, respectively) in their bulk forms. The energetic stability of the codoping (S, Se) sites with (C, Si), (N, P), (P, As), (N, As) and (F, F), respectively in the MoSSe janus monolayer is evaluated by the calculation of their corresponding formation energies, which represent the change in the energy. However, the formation of a material can be established from its components in their respective stable structures. The computed formation energies are collected in Table 1.

We computed the formation energy of the janus MoSSe monolayer codoped by elements, such as C, Si, N, P, As, and F, to determine the most favourable phase. Among all the possible substitutional atoms at (S, Se) host atoms in the janus MoSSe monolayer, the codoping of MoSSe janus monolayer with (F,F) atoms instead of (S, Se) anion atoms, was found to have the lowest energy compared with the others (see Table 1). It is the most energetically favourable compared with other codoped elements that are covalently bonded to the Mo atom. This can designate the suitable energetic stability of this monolayers by proposing the feasibility of its experimental growth. This was proposed by

Table 1
Formation energy (unit in eV) of different substitutional codopants (C, N, Si, P, As, and F) at (S, Se) host atoms of janus 2H-MoSSe monolayer with a 3 × 3 supercell (MoSSe-CSi, MoSSe-NP, MoSSe-NAs, MoSSe-PAs, and $MoSSeF_2$).

MoSSe-CSi	**3.86**
MoSSe-NP	**3.13**
MoSSe-NAs	**2.56**
MoSSe-PAs	**2.11**
MoSSe-F_2	**0.95**

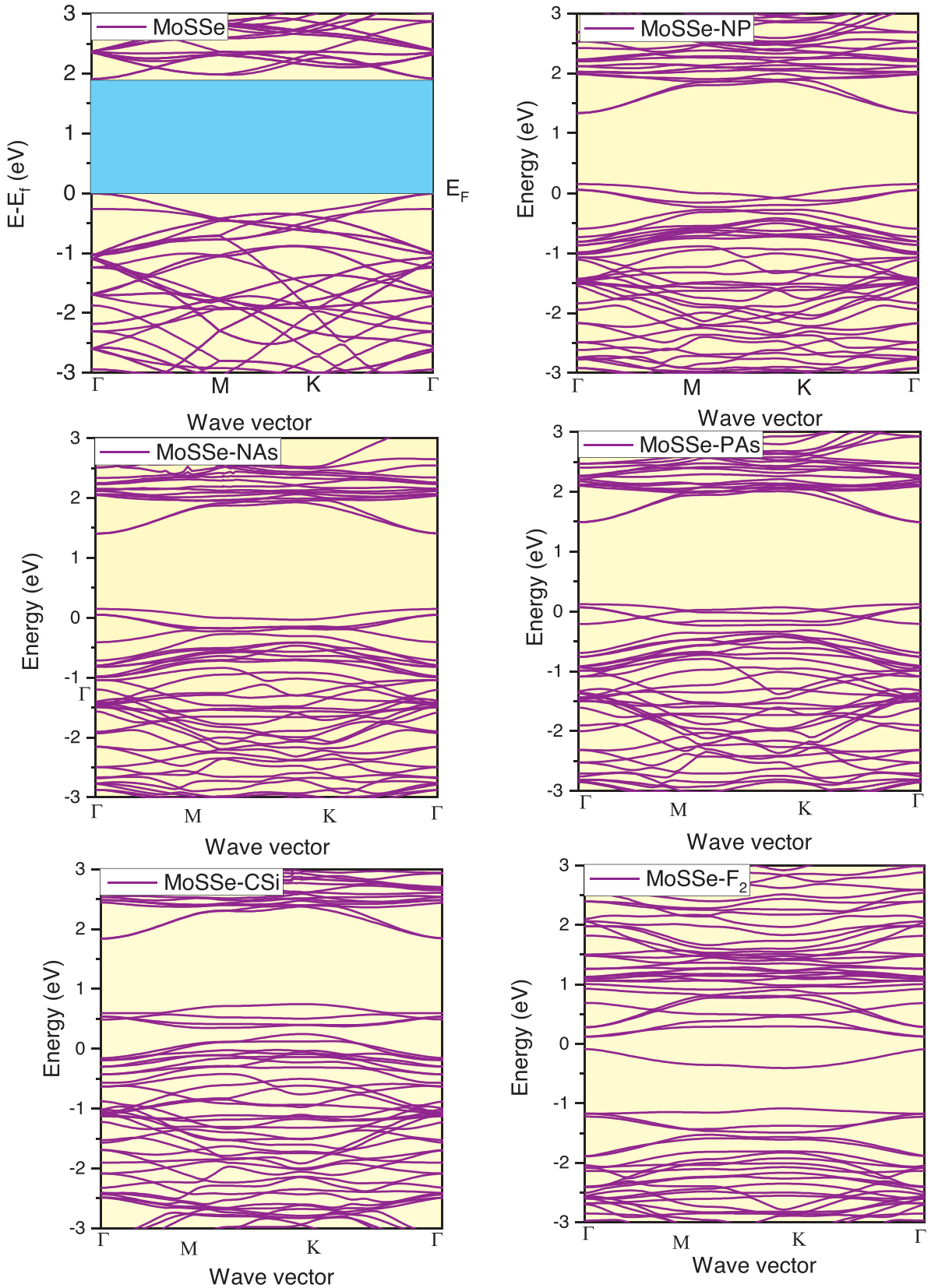

Fig. 2. Band structures of 2H-MoSSe 3x3 supercell janus- monolayer and its codoping S and Se sites with (C, Si, N, P, As, and F). The electronic structures show a shift of the upper valence bands above E_F for C/Si, N/P, N/As, P/As substituted instead of S/Se anion atoms in MoSSe-janus-monolayer leading to p-type conductive system, whereas the impact of halogen F atom taking place instead of S/Se atoms of the host material MoSSe-janus monolayer induces a shift of the lower conduction bands downward E_F with n-type conductive material. The MoSSe-janus-monolayer indicates a semiconducting character with a direct band gap of 1.85 eV between the downward conduction band and the upward valence band. Note that the direct band gap transition is owing to the zone-folding along the Γ- Γ-direction.

the previous experimental investigation [35] and predicted by a previous theoretical calculation [36] for the MoS_2 monolayer. However, the variation in magnitude of the formation energy of the codoped systems depends on the difference in the covalent and ionic bonding between the non-metallic elements, Mo atom, and (S,Se) anion atoms, as well as in the charge transfer between these elements and the Mo atom. Our results indicate that the replacement of both S and Se atoms with non-metallic elements is a good way of designating a janus MoSSe monolayer with a p-type or an n-type character.

Electronic properties and charge densities of the pure janus MoSSe monolayer and its counterpart co-doped with non-metallic elements of C, N, Si, P, As, and F

The electronic band structures of the pristine janus MoSSe monolayer and its counterpart co-doping S and Se sites with non-metallic elements (C, Si, N, P, As, and F) are shown in Fig. 2. The energy-level separation between the conduction band minimum (CBM) and the valence band maximum (VBM) are computed over the full Brillouin zone of the hexagonal structure. The position of Fermi level is set at VBM. Apparently, the pure janus 2H-MoSSe monolayer with a 3 × 3 supercell has a semiconducting character with a direct band gap transition of 1.85 eV from the VBM to the CBM (Γ-Γ) (see Fig. 2). These results agree reasonably well with those quoted from the previous experimental and theoretical works [25,29–31]. The computed energy band gap of 1.85 eV is in reasonably accordance with the experimental optical band gap of 1.80 eV [25]. It was previously reported that the pure MoSSe bulk material owns an indirect band gap transition of 1.5 eV through the Γ-K direction [31]. Hence, a transition emerges from the indirect gap to the direct gap when undergoing from the MoSSe bulk material to the janus monolayer. According to the previous theoretical works [13,16], the bulk MoS_2 semiconductor possesses also an indirect band gap of approximately 1.2 eV. The semiconducting bulk MoSSe is made up of a bonding- van der Waals type between S-Mo-Se units [18–26]. Each of these stable structural cells is composed of two hexagonal upper and lower planes of S and Se atoms and of the medium hexagonal plane of Mo atoms that have a coordination of covalent bonding with both S and Se atoms in a trigonal prismatic pattern (see Fig. 1). Note that, for the bulk system, the VBM shifts from halfway along the Γ-K line toward K. By applying a zone-folding effect, we can generate the 2D electronic states of the janus MoSSe monolayer by a subset of the bulk band structure with quantised in-plane momenta. It means that the momenta positioned in planes orthogonal to the Γ-K or K-M directions in the Brillouin zone. The pristine janus 2H-MoSSe monolayer with a 3 × 3 supercell undergoes a crossover to a direct band gap semiconductor. For janus MoSSe monolayer with a 3 × 3 unit cell, the band structure had a quantum confinement that induces an alteration from the indirect gap of a bulk value of 1.48 eV to a direct one of 1.85 eV for monolayer [25]. Thus, MoSSe bulk crystal undergoes a crossover through an indirect gap to a direct gap semiconductor in the monolayer limit.

To reveal the alteration of the band structures of the janus 2H-MoSSe monolayer co-doping S and Se sites with a p-type ((C, Si), (N, P), (N, As) and (P,As)) and an n-type (F, F) elements, we analysed in detail the nature of the electronic band structures. We then examined the viability of p-type doping acquired by substituting the S/Se anion atoms with elements from groups IV and V of the periodic table, namely, C, Si, N, P, and As, respectively. In contrast, for the n-type character, the F atom was chosen as the replacement instead of the S/Se atoms. The band structures of all 2D materials under study, such as the pristine janus 2H-MoSSe monolayer with a 3 × 3 supercell and its counterparts co-doped with non-metallic elements (such as MoSSe-CSi, MoSSe-NP, MoSSe-NAs, MoSSe-PAs, and $MoSSeF_2$), are induced chiefly from the 4*d* orbitals of Mo and from the 3*p* or 4*p* states of S or Se in the janus MoSSe monolayer, as depicted in Fig. 2. These states of the pristine monolayer can be hybridised with the sp states of co-doped non-metallic elements near the VBM and the CBM above and below E_F. This can be reflected by the hybridisation between the 2*p*/3*sp*/4*p* states of the C, N, Si, P, and As elements and S/Se-3*p*/4*p* states as well as the 4*d*/5*s*-orbitals of Mo atoms in the monolayer. This can however create a covalent bonding between the non-metallic elements (C, Si, N,P, As, S, and Se) and Mo in-plane. As shown in Fig. 2, the shift of the VBM upward E_F for the co-doping S and Se sites with C, Si, N, P, and As in the janus 2H-MoSSe monolayer having 3x3 supercell, was a result of the charge transfer between the S (C, Si, N, P, and As) and the Mo atoms (C-S, Si-Se, N-Mo, P-Mo, and Mo-As bonding). This could then induce the breaking of the degeneracy of the CBM and VBM at the Brillouin zone of the hexagonal structure. For F element substituted by S and Se atoms in the janus MoSSe monolayer, an n-type is present in the janus MoSSe monolayer. This is due to the fact that F atom has one supplementary p electron compared with S or Se atoms. It is well known that the p-type atom affects the displacement of the upper valence states above E_F and the n-type doping atom affects the shift of the lower conduction states beneath E_F level (see Fig. 2).

It is well remarkable that the upper valence bands were pulled upward E_F along the M − K − direction, leading to a janus MoSSe monolayer with a p-type character, whereas the CBM shifted downward E_F with an n-type character in the janus MoSSe monolayer (see Fig. 2). Accordingly, the C, N, Si, P, As, and F atoms form a covalent bonding with the S or Se atom in the janus 2H-MoSSe monolayer and the symmetric structure was broken, leading to a p-type or an n-type character for the doping of the MoSSe monolayer depending on the doping effect [46–51]. The bands nearby E_F have rather a flat shape, as anticipated via the *d*-orbitals of the Mo electrons at those energies. Apparently, the degeneracy of both the upper valence states and the lower conduction states was lifted in the region of E_F in both the Γ-M and the M − K direction. This can result in the enhancement of the overlap between the S/Se-3*p*/*4p* and the C-, N-, Si-, P-, and F-p orbitals above and underneath E_F. Note that the electrons were conveyed via the C, N, Si, P, and F atoms to the Mo atom, confirming the strong localisation of the electrons in-plane. The increase in the supercell of the janus MoSSe monolayer in-plane can be associated to the quantum confinement impact, besides the covalency and charge transfer, which can vary between the Mo and S/Se elements and the co-doped non-metallic elements, compared with those of the host material. As clearly noted, the 4*d* states of the Mo atom degenerated into a bulk structure [26], whereas a small separation occurred in the janus monolayer. This type of behaviour, emerging from the 4*d*-states interaction in the janus MoSSe monolayer, may also induce in other layere d TMDCs.

The origin of the electronic band structure can be discerned via the density of states (DOS) under the co-doping effect on the janus MoSSe monolayer. Furthermore, we discuss the codoping S and Se anions of the host MoSSe monolayer with non-metallic elements (such as MoSSe-CSi, MoSSe-NP, MoSSe-NAs, MoSSe-PAs, and $MoSSeF_2$) having sp states. The codoping effects on the janus MoSSe monolayer are elucidated from the variation of the number of states close to E_F, as depicted in Fig. 3. This can play a major role on the alteration of the VBM and CBM nearby E_F. Note that the number of states in the total and atomic project DOS of janus MoSSe monolayer is modified by inserting in the host material some selected non-metallic elements of the periodic table, from column IV to column VIII. The total DOS of the pristine janus MoSSe monolayer and the extrinsic semiconductors with a p- or an n-type character are depicted in Fig. 3. The electronic DOS can be separated into three sets of states, disjoined by a band gap for the free-standing janus MoSSe monolayer, as seen in Fig. 3. In the first section, the electronic states of the DOS around −6 eV are essentially owing to the set of states composed of 3*p*/4*p* orbitals of S/Se atoms as well as 4*p* orbitals of Mo atom and are together strongly hybridized. In the next set above E_F, the main participation of CBM is arising from the 4*d*/*5s* states of Mo atom , and is separated by a band gap from the second group of VBM below E_F for the pristine janus 2H-MoSSe monolayer having a 3 × 3 supercell. The DOS shows that the Mo-4*d* and S/Se-3*p*/4*p* states contribute dominantly to the DOS around E_F, besides to the S or Se sites

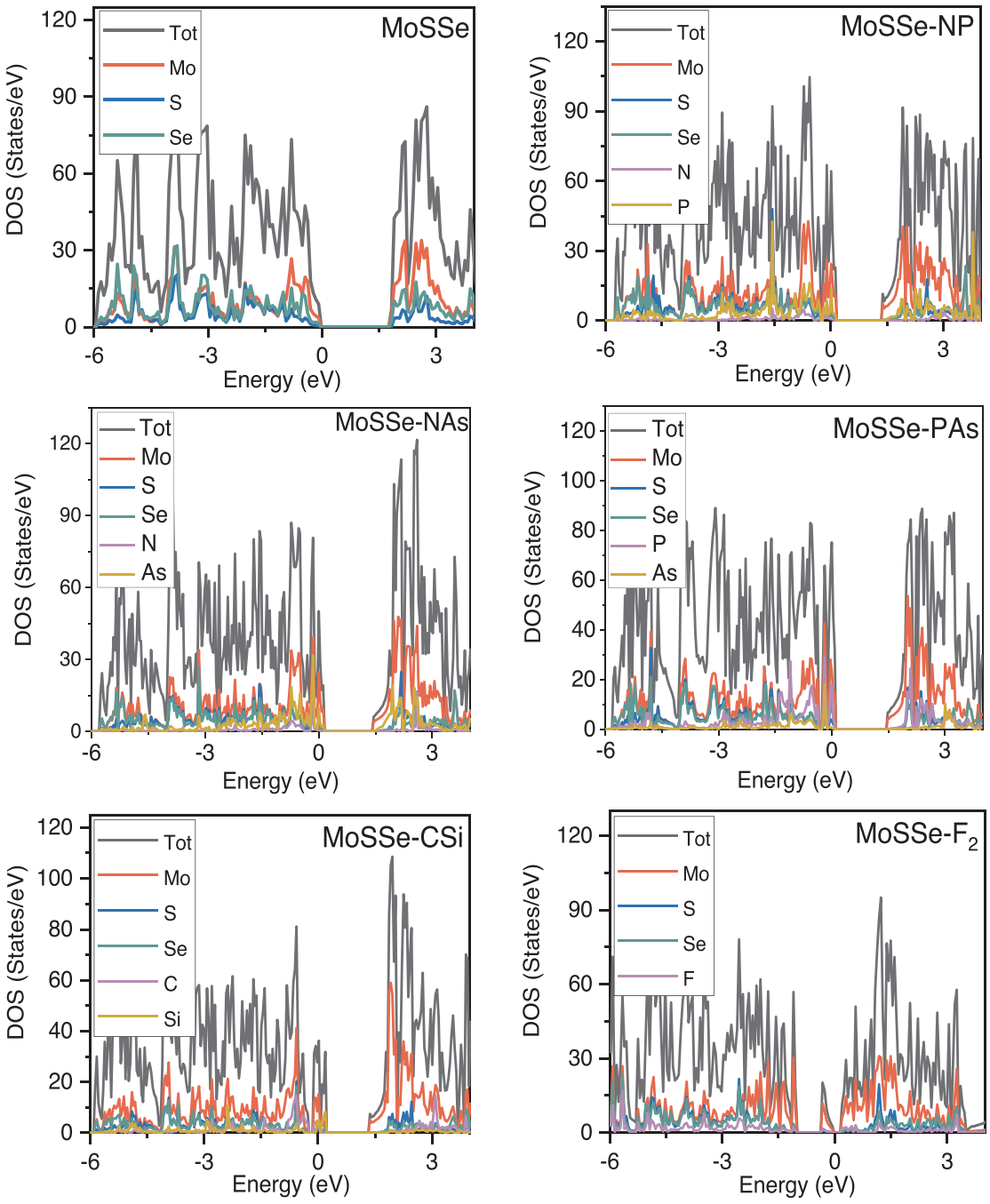

Fig. 3. Total and atomic projected density of states on C, Si, N, P, As, and F for 2H-MoSSe 3x3 supercell janus- monolayer and its co-doping S and Se sites with C, Si, N, P, As, and F elements.

that are replaced in the janus MoSSe monolayer by C, Si, N, P, As, and F elements. It is also clearly observed that the CBMs are shifted below E_F when (F, F) are replaced by S and Se atoms as compared to the pristine monolayer. This is due mainly to the addition of one more electrons in F atom in comparison with S/Se atoms, yielding to n-type doping nature. Note that the lower valence bands are changed and their energy levels were split in the range of −6 to 0 eV. This can be related to the effect of the C, N, Si, P, As, and F elements codoped into the janus MoSSe monolayer, in comparison with the DOS of host material, namely, the freestanding janus MoSSe monolayer (see Figs. 2 and 3).

The total and atomic projected DOS plots of the C, Si, N, P, and As atoms doped into the pure janus MoSSe monolayer show a displacement of the upper valence states above E_F (see Fig. 3). This can be caused by the increase in the valence electrons of the doped atoms in the host system, and, thereby, the concomitant electronic states were relocated above E_F. This is a good indicator of an induced p-type janus MoSSe monolayer. The valence band located at −4.9 eV to 1.7 eV originated from the S-3*p*, Mo-4*d*, C-2*p*, N-2*p*, P-3*p*, and Si-3*p* states that were shifted above E_F for conduction band to a p-type character based on the janus MoSSe monolayer. In the conduction band, the region from 2.0 eV to 4.5 eV consisted of hybridized states composed of Mo-5 *s*, S/Se-s, and C, N, P, As, and Si s/p orbitals. Clearly, several sharp peaks appeared in the DOS near E_F at (-3.8, −2.5, and 1.5 eV), (-3.6, −2.7, −1.8, and 0.6 eV), (-4.1, −3.7, −1.5, and 0.4 eV), and (-5.8, −3.1, −2.7, and −0.6 eV) for the janus MoSSe monolayer doped with C, N, P, As, and Si atoms, respectively. We noted that the first peak located downward E_F came from the p states of C, N, P, As, and Si atoms between −2.7 and −0. 6 eV, respectively. It was clearly observed that

feature peaks are located above E_F for the DOS near 0.4–3.5 eV in the janus MoSSe monolayer co-doped with C, N, P, As and Si atoms, respectively, which is caused by the mixture between the p states of C, N, P, Si, As, S, and Se atoms. In addition, the occupied p-orbital electrons of C, N, P, As, and Si cause a shift in the VBM above E_F. From a theoretical perspective, the replacement of the S or Se atoms with C, Si, N, P, and As atoms will alter the total number of electrons. In comparison with previous theoretical data, the DOS of the janus 2H-MoSSe monolayer showed an upward shift for the VBM above E_F as compared with the pristine case, which was characteristic of p-type behaviour [25]. Fig. 3 shows near E_F that the number of states increases and splits because of the increase of the number of valence electrons in outer-shell of F atom irrespective with S or Se atoms. The VBM located from -6 to -2.5 eV is originating from the mixture of the Mo-*4p*, S/Se-3*p*/4*p*, and F-2*p* states. The CBM positioned between -1 and 2.5 eV is composed of Mo-4*d* and S/Se-3*p*/4*p* states as well as a few contributions from the F-2*p* state. These conduction states are originally shifted downward E_F, whereas the conduction band arising from 2.8 to 3.5 eV consist of the hybridisation between the Mo-*5 s*, S/Se-3*p*/4*p*, and F-2*p* orbitals.

To understand the distribution of molecular orbitals of both pristine and doped MoSSe janus monolayer, we analyzed their charge density. The localization of HOMO-LUMO charge density for pristine MoSSe janus monolayer and localization of molecular orbitals near E_F of MoSSe single-layer doped with F, C/Si, N/P, N/As, and P/ As elements instead of S/Se are displayed in Fig. 4 (a)-(g). As apparent, the HOMO and LUMO orbitals of pure MoSSe single layer are covalently bonded via *sp*2 hybridisation between S-Mo-Se atoms. It is clearly seen from Fig. 4 (c) that the electrons are transferred from Mo to F atom because of different electronegativity of F and Mo atoms. Thus, the localization of the electron in this n-type semiconductor has convalent character between the F-Mo bonding. Additional examination, of the localization charge density near E_F for C/Si, N/P, N/As, and P/As elements that replace S/Se atoms of MoSSe janus free-standing layer, are exhibited in Fig. 4(d)-(g). It is clear that the localisation of the electrons is significant in the case of C/Si doped into MoSSe janus monolayer comparatively to the other remaining systems. This is due mainly to the strong covalent character in the region of C-Mo-Si bonding that can render the system to be p-type extrinsic semiconductor. A similar behavior is present for other systems, as shown in Fig. 4 (e)-(g). It is obvious that the codoping with N, P, As instead of S/Se atoms conducts to a deficient of single electron in S or Se. Thus, a small localisation of charge close to S/Se and bump of charges on foreigner codoped elements in MoSSe monolayer, is yielding to p-type extrinsic semiconductor.

Optical properties of the janus MoSSe monolayer and its counterpart co-doped with non-metallic elements (C, Si, N, P, As, and F)

The information regarding the optical properties is provided from the interaction of the electromagnetic radiation with a material, which can be described via an important key component, the so-called dielectric function. This component is connected to the electronic band structures of a solid, and it can be examined using optical spectroscopy. In this case, the dielectric function is composed of two terms, namely, the real and imaginary parts. The relation $\varepsilon(\omega) = \varepsilon_1(\omega) + i\varepsilon_2(\omega)$ is expressed via the response of a material to the photon spectrum.

The real part of the dielectric function of the considered systems is given by :

$$\varepsilon_1(\omega) = 1 + \frac{2}{\pi} P \int_0^{\infty} \frac{\hat{\omega}\varepsilon_2(\hat{\omega})}{\hat{\omega}^2 - \omega^2} d\hat{\omega} \quad (1)$$

The imaginary part of $\varepsilon(\omega)$ is calculated as follows:

$$Im[\varepsilon^{jj}(\omega)] = \frac{e^2\hbar^2}{\pi m^2\omega^2} \sum_{v,c} |\langle \psi_c | \hat{e_j}.\, P | \psi_v \rangle|^2 \delta(E_c - E_v - \hbar\omega) \quad (2)$$

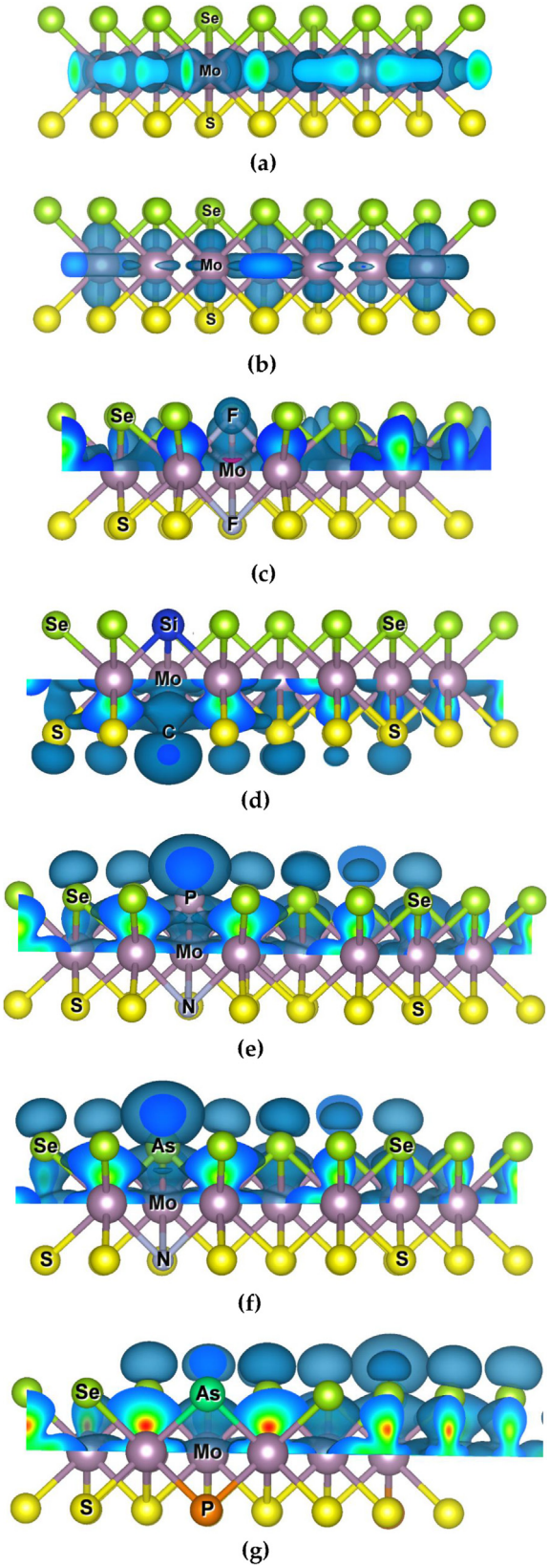

Fig. 4. Localization of charge density (a) HOMO- MoSSe janus monolayer, (b) LUMO-MoSSe janus monolayer, (c) charge density of fluorine doped into MoSSe near E_F, (d), (e), (f), (g) charge density near E_F of MoSSe janus free-standing layer where S/Se elements are replaced by C/Si, N/P, N/As, and P/As atoms, respectively.

Where, the unitary vector $\widehat{e_j}$ is related to the direction of the external electromagnetic field of energy$\hbar\omega$. The vacant and filled eigenfunctions states of the material are denoted by ψ_v and ψ_c, respectively, while E_v and E_c describe the associated energies. e and m indicate the charge and mass of the bare electron, respectively, whereas the momentum operator is characterized by p. Based on the optical spectra of the real and imaginary terms of $\varepsilon(\omega)$, other optical spectra can be evaluated, the so-called absorption coefficient, reflectivity, and energy loss function [42]. In our case, all optical spectra of the hexagonal structures are computed in plane (xx direction) and out of plane (zz direction). The optical absorption coefficient is written by the relationship of the imaginary part of the dielectric function (2).

The reflectivity $R(\omega)$ as a function of the photon energy is provided by using the optical parameters, as the refractive index $n(\omega)$ and the extinction coefficient $k(\omega)$, as denoted by the following expression:

$$R(\omega) = \left|\frac{\tilde{n} - 1}{\tilde{n} + 1}\right| = \frac{(n-1)^2 + k^2}{(n+1)^2 + k^2} = \left|\frac{\sqrt{\varepsilon(\omega)} - 1}{\sqrt{\varepsilon(\omega)} + 1}\right|^2 \quad (3)$$

The energy loss function $L(\omega)$ is expressed by:

$$L(\omega) = -\mathrm{Im}\left(\frac{1}{\varepsilon}\right) = \frac{\varepsilon_2(\omega)}{\varepsilon_1^2(\omega) + \varepsilon_2^2(\omega)^2} \quad (4)$$

The examination of the optical absorption coefficient provides a clear elucidation of the electronic structures of the systems under study. The optical spectra calculations of the pristine janus MoSSe monolayer and its counterparts co-doping S and Se sites with sp-elements (such as MoSSe-CSi, MoSSe-NP, MoSSe-NAs, MoSSe-PAs, and $MoSSeF_2$) are evaluated via the real and imaginary parts of the dielectric functions. The optical absorption coefficient of the pristine and co-doped janus MoSSe monolayer are computed in the photon energy regime of 0–20 eV. Thus, to gain a keen understanding of the behaviour of the pure janus 2H-MoSSe monolayer and its counterpart co-doping S and Se sites with sp- anion elements, we calculated the optical absorption spectra with polarisation vectors parallel ($E_\parallel$) and perpendicular ($E_\perp$) to the xy-plane, which will provide the optical absorption spectra $\alpha\|^{(\omega)}$ and $\alpha^{\perp(\omega)}$, respectively. Remarkably, the shapes of the optical absorption spectra of the in-plane ($E_\parallel$) and perpendicular-to-plane ($E_\perp$) polarisation vectors are dissimilar at low photon energy for both pure and co-doped janus MoSSe monolayer. Hence, the optical absorption coefficient spectra between the in-plane ($E_\parallel$) and the out-of-plane polarisation component ($E_\perp$) are anisotropic for all the materials under study at photon energies less than 11.5 eV, whereas their shapes became isotropic above 13 eV, as depicted in Fig. 5. The optical absorption spectra for all systems in the in-plane ($E_\parallel$) and out-of-plane ($E_\perp$) polarisation vectors display quite comparable spectral dispersion at high photon energies (see Fig. 5).

The starting of optical absorption response of janus MoSSe monolayer is indicated at photon energy of the direct band-gap transition of 2 eV. However, an alteration from the visible to the UV is assigned at low photon energy with an insignificant blue shift of the resonances (Fig. 5). The positions and magnitude of the spectral optical peaks of the janus MoSSe monolayer are ~2, and 7.5 eV, respectively, in the in-plane polarisation vector ($E_\parallel$). Also, the positions of the two feature peaks in the out-of-plane polarisation vector ($E_\perp$) are close to 10.2 and 11.8 eV, exhibiting an inter-band transition. Note that the highest peak located at 10.2 eV is due to the strong excitonic effect at the uncommon larger energies (see Fig. 5). The absorption peaks at 2.5 and 5.2 eV in both the in-plane and the out-of-plane vector coincide the two absorption resonances and are designated to the direct-gap material. The transitions resulting from the valence states below E_F to the conduction states upward E_F are in accordance with the preceding theoretical works [48]. These features suggest that the janus MoSSe monolayer has a direct-gap semiconductor compared with the bulk state [25], which has an indirect band gap. As discussed previously, it is attributed to the direct-gap luminescence [25]. As mentioned previously, the computed optical absorption spectra of the in-plane and out-of-plane polarisation vectors for the MoSSe system [26] were significantly anisotropic in their underneath-energy span (less than10 eV) and became isotropic in their upper-energy interval, which is quite analogous to our results. Moreover, the strong absorption power of these materials is inferred in the near infrared and visible energy ranges.

From the analysis of the optical spectra, janus MoSSe monolayer co-doped with C, N, Si, P, As, and F atoms, show a lower absorption peak that shift systematically to low energies, and it is weak compared with the pure monolayer (see Fig. 5). The optical absorption for the janus MoSSe monolayer codoped with p-type (C, N, Si, P, and As) and n-type (F) elements at S and Se sites, clearly illustrate a metallic behaviour and the absorption starts from zero photon energy. The first spectral peaks are due to the electron transition from S or Se 3*p*/4*p* (valence band) to C, N, Si, P, As, and F-sp (conduction band) in addition to the Mo 4*d*/5*s* states. Remarkably, the shapes of the optical absorption spectra for the in-plane ($E_\parallel$) and perpendicular-to-plane ($E_\perp$) polarisation vectors are almost alike for the codoping with (C, N, Si, P, and As) and act as p-type conducting (see Fig. 5). This situation can be related to the bonding interactions between these codoped sp-elements in the janus MoSSe monolayer. However, the situation is reversed for the pristine janus MoSSe monolayer that composes the atomically thin material and represents a practical light-emitter (see Fig. 5). As a result, we conclude that an alteration in the optical absorption spectra emerges under the doping effect in-plane with the janus MoSSe monolayer. Clearly, the optical spectra of the in-plane polarisation vector had two peaks for all codoped systems. The first consisted of a sharp, well-defined peak around 0.5–3 eV, and the second peak is around 3.5–6 eV for these systems. There is no absorption in the range of 15–20 eV because the energy of the incident photons is insignificant. The optical absorption spectra of the out-of-plane polarisation vector had two sharp peaks in all materials located between 5 and 9.5 eV. The starting value for the in-plane polarisation vector was ~0.5 eV in the janus MoSSe monolayer co-doped with C, Si, N, P, As, and F atoms. It is well remarkable that the optical spectra of the out-of-plane polarisation vector shifted to high photon energy when going from the janus MoSSe monolayer doped with C to F atoms. The optical absorption of the out-of-plane polarisation vector exhibited a red shift for the janus MoSSe monolayer co-doped with C, N, Si, P, As, and F atoms. This red shift in the optical absorption corresponded to either the p-type or the n-type character of the janus MoSSe monolayer, and this depended on the type of doping element.

The results showed that tunable optical properties could be achieved by altering the codoping C, N, Si, P, As, and F elements at S and Se sites of the janus MoSSe monolayer. Unlike those in previous works [26,32,33], the absorption spectra for the monolayers MoS_2, $MoSe_2$, and WS_2 are splitting into a lower energy span, which is governed by excitonic transitions with a nearly weak absorption. Our results corroborate the previous photoemission measurements [26]. Additionally, the optical absorption spectra of the MoS_2, $MoSe_2$, WS_2, and WSe_2 monolayers were found to have a low absorption at low energy owing to the excitonic transitions and a significant absorption at higher energies was observed in the MoS_2 monolayer [47]. The computed results were consistent with the X-ray photoemission measurements [49], where five peaks showed strong S/Se3*p*/4*p*-Mo4*d* hybridisation. Thus, a strong transition due to the Mo 4*p* band can form an absorption around 14 eV [26,33].

Reflectivity represents an important feature to exhibit the optical behavior of materials. The normal incident reflectivity $R(\omega)$ reveals the linear optical response between the maximum valence states and the lower conduction states. The spectral features of reflectivity at the photon energy regime of 0–20 eV are displayed in Fig. 6. The reflectivity spectra of the in-plane ($E_\parallel$) and out-of-plane ($E_\perp$) polarisation vectors showed a quite analogous spectral dispersion for larger energies for all systems (see Fig. 6). Apparently, the reflectivity was approximately 0.1 and 0.2 for both the parallel and perpendicular polarisation

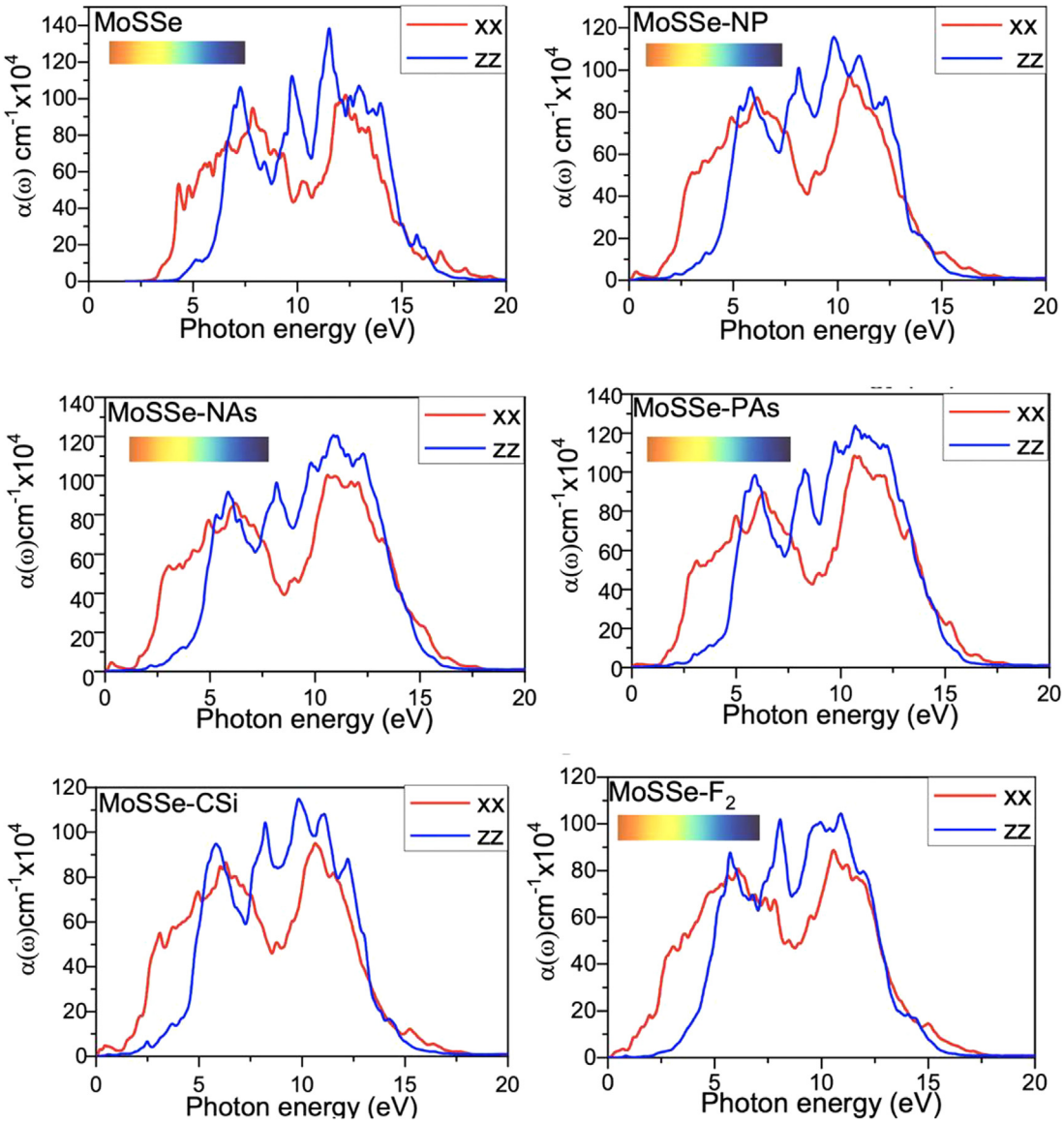

Fig. 5. Optical absorption coefficient of 2H-MoSSe 3x3 supercell janus- monolayer and its co-doping S and Se sites with C, Si, N, P, As, and F elements.

vectors at zero photon energy for the janus MoSSe monolayer, as illustrated in Fig. 6. Furthermore, a pronounced reflectivity is detected in the moderate visible-UV regime (0 → 7.5 eV). It is worth nothing that spectral peaks of reflectivity emerged in the UV light regime (9.5 → 14.5 eV). The reduced reflectivity developed in the range of 15 → 20 eV for the pristine janus MoSSe monolayer. Importantly, upon the doping with non-metallic elements (C, Si, N, P, As, and F), the reflectivity exhibited a pronounced peak in the energy interval between 10 and 14.5 eV, and this may be due to the p-type or n-type extrinsic semiconductor nature of these 2D materials. A diminished reflectivity spectral peak is found in the UV regime (5 → 12.5 eV) for all doped systems (see Fig. 6). Note that the reflectivity was recorded at zero photon energy for both parallel polarisation (0.1, 0.17, 0.2, 0.25, 0.17, and 0.15) and perpendicular polarisation vector (0.2, 0.52, 0.5, 0.45, 0.49, 0.47, 0.51, and 0.44) of the pure and co-doped systems, such as the MoSSe, MoSSe-NP, MoSSe-NAs, MoSSe-PAs, MoSSe-CSi, and MoSSe-F_2 materials, respectively. A drop in the reflectivity spectral peak was exhibited in the high photon energy. Interestingly, the transitions principally emerged from the chalcogen S/Se p states and Mo-4*d*/5*s* states mixed with the sp states of codoped elements. The prominent spectral reflectivity at a photon energy less than 1.5 eV indicates the conducting behavior of the janus MoSSe monolayer co-doped with C, Si, N, P, As, and F atoms, respectively in the low photon energy regime. From a Drude-type inspection [37], these co-doped systems showed a conductive behaviour with either a p-type or an n-type character acquired in the near infrared and visible reflectivity spectra at low energy regimes. However, the reflectivity spectra of the pristine janus MoSSe monolayer were approximately analogous to those of the MoS_2 monolayer [47], which was confirmed from the UV and vacuum UV regions [33].

The electron energy loss function $L(\omega)$, that is depicted in Fig. 7, was employed to procure the energy loss of a prompt electron conveying the medium. The $L(\omega)$ spectra exhibited peaks owing to the plasma resonance at the plasma frequency ω_P. In the case of the co-doped elements (C, Si, N, P, As, and F) instead of S and Se atoms into the janus MoSSe monolayer, the first peak of the energy loss function is weak at low photon energy in comparison with the pure janus MoSSe monolayer, whereas the loss function emerged around 12.5 eV for the pure monolayer. It can clearly be seen that the first weak plasmon peaks $L(\omega)$ are between 2.5 and 5.5 eV for the in-plane polarisation vector for both for the pure janus MoSSe monolayer and its counterpart co-doped with C, Si, N, P, As, and F atoms at S and Se sites. As illustrated in Fig. 7,

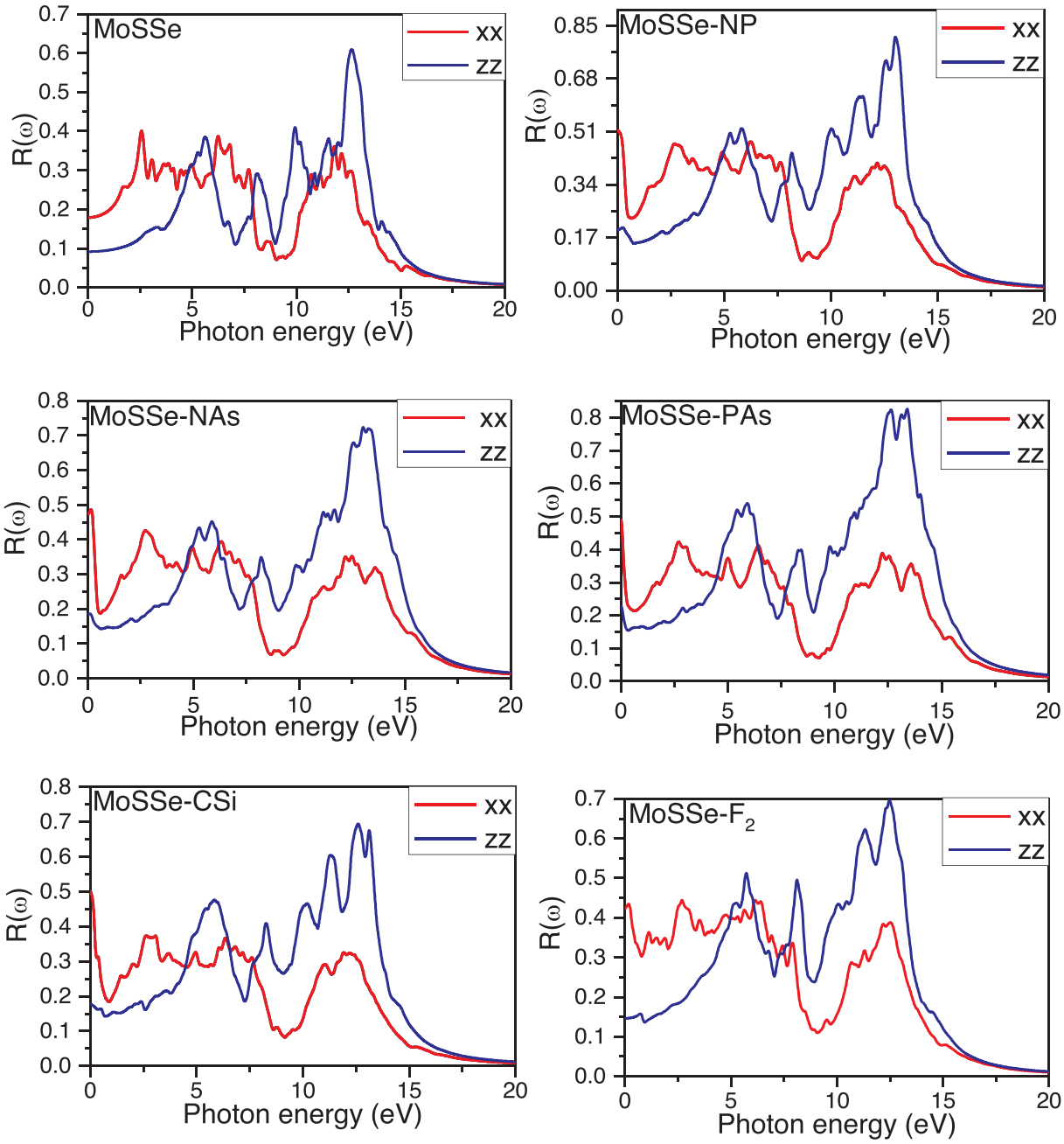

Fig. 6. Reflectivity of 2H-MoSSe 3x3 supercell janus- monolayer and its co-doping S and Se sites with C, Si, N, P, As, and F atoms.

the second intense sharp peaks of the energy loss function are located between 11 and 13 eV for both parallel and perpendicular polarisation of light for these 2D materials. A strong anisotropy occurred for all systems in this photon energy regime. However, the energy loss vanished around the photon energy regime of 15–18 eV. By analysing the variations of the electron energy loss function of the janus MoSSe monolayer, we obtained a result that showed a shift of the plasmon peak at 15.3 eV [48,49]. The electron energy loss function shifted to a lower energy after the janus MoSSe monolayer was co-doped with C, Si, N, P, As, and F) elements. The tailoring of the physical properties indicates that these two-dimensional materials can be promising in the fabrication of the most feasible electronic devices.

Conclusion

In this work, the computed electronic structures and physical behaviors of pristine janus 2H-MoSSe monolayers, having a 3 × 3 supercell, and its co-doping S and Se sites with C, Si, N, P, As, and F atoms, are carried out by means of plane-wave pseudopotential method. The electronic band structures and their corresponding DOS indicated that the free-standing janus MoSSe monolayer has a semiconducting nature, with a discerned direct band gap transition. Moreover, the upper valence and lower conduction bands of the DOS exhibited a significant contribution from Mo-4*d* and S/Se-3*p*/4*p* around E_F. A hybridization between the sp states of the substituted C, Si, N, P, As, and F anion elements at S/Se sites and the 4*d* orbitals of Mo yielded a covalent bonding in the janus monolayer. From the calculated DOS, a shift in the upper valence band and lower conduction band was found and this depends on the type of co-doping element into janus MoSSe monolayer. It was surmised that the replacement of S/Se atoms with sp-non-metallic elements enables us the tailoring of the electronic properties of janus MoSSe monolayer with the occurrence of either p-type or

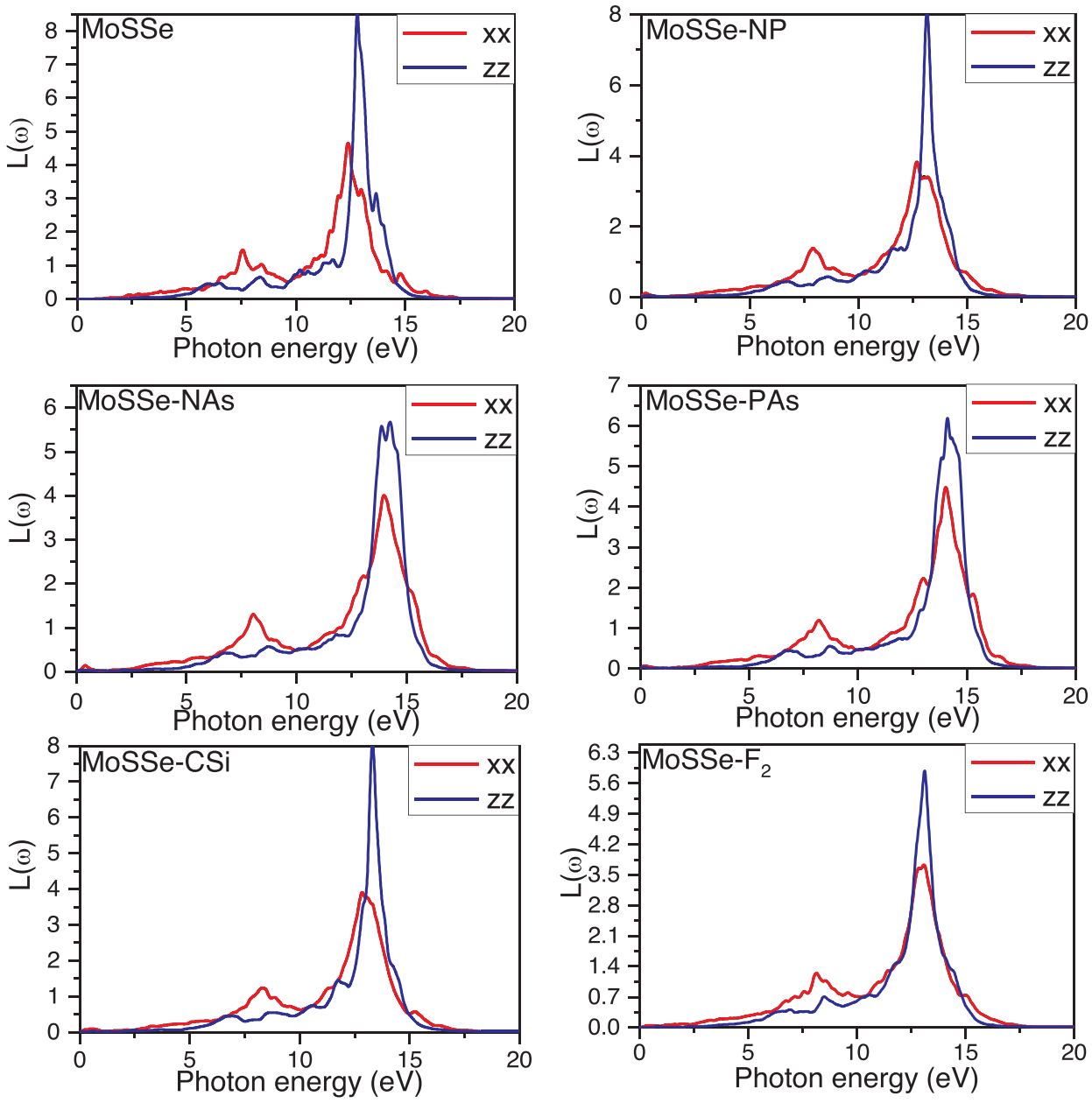

Fig. 7. Energy loss function of 2H-MoSSe 3x3 supercell janus- monolayer and its co-doping S and Se sites with C, Si, N, P, As, and F non-metal elements.

n-type conductivity. The resulting electronic structures illustrated that C, Si, N, P and As atoms co-doped into S and Se host atoms of the janus MoSSe single-sheet, may imply a shift of the valence band maximum above E_F. This can hence indicate an extrinsic p-type semiconductor. The displacement of the conduction band minimum below E_F of the co-doping S and Se anion sites of the pristine janus MoSSe monolayer with (F, F atoms), exhibited n-type behaviour. Note that the co-doping S and Se anion atoms with sp- elements affected considerably the electronic structures of MoSSe monolayer because of the charge transfer between the substituted anion elements and Mo atom of the free-standing monolayer. From the analysis of the optical spectra, it was found that the absorption starts from zero photon energy in janus MoSSe monolayer substituted with C, Si, N, P, As, and F atoms at S and Se sites, leading to p-type or n-type characters. The positions and intensity peaks located in the optical spectra of the janus MoSSe monolayer were determined for both in-plane and out-of-plane polarisation directions. It was acquired that the shapes of the optical spectra are anisotropic in the two polarisation directions. The optical absorption for the polarisation parallel to the x-y plane illustrated that the janus MoSSe monolayer could vary spectrally from the visible to the UV at low photon energy range. Moreover, the reflectivity spectra showed an augmentation at the zero photon energy due to the co-doping impact on the pure janus MoSSe monolayer with sp-anion elements. Interestingly, a substantial reflectivity was developed at low-energy window from 0 up to 12.5 eV. It is surmised that the energy loss function has a pronounced plasmon peak $\underline{L}(\omega)$ appearing around 13 eV. The present calculations illustrate that the replacement of S/Se atoms with sp anion elements is suitable for tailoring the electronic and optical behaviors of the janus MoSSe monolayer. From our theoretical contribution, the distinctive electronic features of janus MoSSe monolayer, may enable extensive applications of such atomically thin materials. This could provide new technological road maps, such as catalysis, energy storage, humid sensors, and field transistor effect devices for 2D materials.

CRediT authorship contribution statement

F. Barakat: Conceptualization, Data curation, Formal analysis, Investigation, Methodology, Project administration, Validation, Visualization, Writing - original draft, Writing - review & editing. **A. Laref:** Conceptualization, Formal analysis, Investigation, Supervision, Validation, Writing - review & editing. **M.S. AlSalhi:** Writing - review & editing. **S. Faraji:** Supervision, Validation, Writing - review & editing.

Declaration of Competing Interest

The authors declare that they have no known competing financial interests or personal relationships that could have appeared to influence the work reported in this paper.

Acknowledgement

The authors are grateful to the Deanship of Scientific Research, King Saud University for funding through Vice Deanship of Scientific Research chairs.

References

[1] Novoselov KS, Geim AK, Morozov SV, Jiang D, Zhang Y, Dubonos SV, et al. Electric field effect in atomically thin carbon films. Science 2004;6:666.
[2] Jariwala D, Sangwan VK, Lauhon LJ, Marks TJ, Hersam MC. Emerging device applications for semiconducting two-dimensional transition metal dichalcogenides. ACS Nano 2014;8:1102–20.
[3] Bhimanapati GR, et al. Recent Advances in Two-Dimensional Materials Beyond Graphene. ACS Nano 2015;9(12):11509–39.
[4] Baugher BW, Churchill HO, Yang Y, Jarillo-Herrero P. Optoelectronic devices based on electrically tunable pn diodes in a monolayer dichalcogenide. Nat Nanotechnol 2014;9:262–7.
[5] Pospischil A, Furchi MM, Mueller T. Solar-energy conversion and light emission in an atomic monolayer pn diode. Nat Nanotechnol 2014;9:257–61.
[6] Pradhan NR, et al. Hall and field-effect mobilities in few layered p-WSe2 field-effect transistors. Sci Rep 2015;5:8979.
[7] Padilha JE, Peelaers H, Janotti A, Van de Walle CG. Nature and evolution of the band-edge states in MoS_2: From monolayer to bulk. Phys Rev B 2014;90:205420–5.
[8] Fan XL, Yang Y, Xiao P, Lau WM. Site-specific catalytic activity in exfoliated MoS_2 single-layer polytypes for hydrogen evolution: basal plane and edges. J Mater Chem A 2014;2:20545–51.
[9] Dajin C, Song L, Huanhuan L, Can L, Lei L, Yinyan G, et al. The effects of local bond relaxations on the electronic and photocatalysis performances of nonmetal doped 3R–MoS_2 based photocatalyst: density functional theory. Mater Res Express 2017;4:035908.
[10] Chou SS, Kaehr B, Kim J, Foley BM, De M, Hopkins PE, et al. Chemically Exfoliated Mos2 as near-Infrared Photothermal Agents. Angew Chem 2013;52:4160–4.
[11] Yang X, Li J, Liang T, Ma C, Zhang Y, Chen H, et al. Antibacterial Activity of Two-Dimensional Mos2 Sheets. Nanoscale 2014;6:10126–33.
[12] Zhang X, Qiao L, Chai L, Xu J, Shi L, Wang P. Structural, mechanical and tribological properties of Mo–S–N solid lubricant films. Surf. Coat. Tech 2016;296:185–1916.
[13] Xu S, Gao X, Hu M, Wang D, Jiang D, Sun J, et al. Microstructure evolution and enhanced tribological properties of Cu-doped WS2 films. Tribol Lett 2014;55:1–137.
[14] Xu J, Chai L, Qiao L, He T, Wang P. Influence of C dopant on the structure mechanical and tribological properties of r.f.-sputtered MoS2/a-C composite. Appl Surf Sci 2016;364:249–56.
[15] Sachs B, Britnell L, Wehling TO, Eckmann A, Jalil R, Belle BD, et al. Doping mechanisms in graphene-MoS2 hybrids. Appl Phys Lett 2013;103:251607.
[16] Yue Q, Chang SL, Qin SQ, Li JB. Functionalization of monolayer MoS2 by substitutional doping: A first-principles study. Phys Lett A 2013;377:1362–7.
[17] Hang Y, Li Q, Luo W, He Y, Zhang X, Peng G. Photo-Electrical Properties of Trilayer MoSe2 Nanoflakes. Nano 2016; 11: No. 1650082.
[18] Nam H, Oh B.R, Chen P, Chen M, Wi S, Wan W, Kurabayashi K, Liang X. Multiple MoS2 Transistors for Sensing Molecule Interaction Kinetics. Sci. Rep. 2015; 5: No. 10546.
[19] Khare HS, Burris DL. Surface and subsurface contributions of oxidation and moisture to room temperature friction of molybdenum disulfide. Tribol Lett 2014;53:329–36.
[20] Gu L, Ke P, Zou Y, Li X, Wang A. Amorphous self-lubricant MoS2-C sputtered coating with high hardness. Appl Surf Sci 2015;33:166–71.
[21] Mutafov P, Evaristo M, Cavaleiro A, Polcar T. Structure, mechanical and tribological properties of self-lubricant W-S–N coatings. Surf Coat Tech 2015;261:7–14.
[22] Gustavsson F, Jacobson S, Cavaleiro A, Polcar T. Ultra-low friction W-S–N solid lubricant coating. Surf Coat Tech 2013;232:541–54827.
[23] Isaeva L, Sundberg J, Mukherjee S, Pelliccione CJ, Lindblad A, Segre CU, et al. Amorphous W-S–N thin films: The atomic structure behind ultra-low friction. Acta Mater 2015;82:84–93.
[24] Joshi RK, Shukla S, Saxena S, Lee GH, Sahajwalla V, Alwarappan S. Hydrogen generation *via* photoelectrochemical water splitting using chemically exfoliated MoS_2 layers. AIP Adv 2016;6:015315.
[25] Chang K, Hai X, Pang H, Zhang H, Shi L, Liu G, et al. Targeted Synthesis of 2H- and 1T-Phase MoS $_2$ Monolayers for Catalytic Hydrogen Evolution. J Adv Mater 2016;28:10033–41.
[26] Jin C, Tang X, Tan X, Smith SC, Dai Y, Kou L. J Mater Chem A 2019;7:1099–106.
[27] Zhang J, Jia S, Kholmanov I, Dong L, Er D, Chen W, et al. Janus monolayer transition-metal dichalcogenides. ACS Nano 2017;11:8192–8.
[28] Wu C, Kim TW, Park JH, An H, Shao J, Chen X, et al. Enhanced tribo electric nanogenerators based on MoS2 monolayer nanocomposites acting as electron-acceptor layers. ACS Nano 2017;11:8356–63.
[29] Liu J, Goswami A, Jiang K, Khan F, Kim S, McGee R, et al. Direct-current triboelectricity generation by a sliding Schottky nanocontact on MoS2 multilayers. Nat Nanotechnol 2018;13:112–6.
[30] Lu AY, Zhu H, Xiao J, Chu CP, Han Y, Chiu MH, et al. Janus monolayers of transition metal dichalcogenides. Nat Nanotechnol 2017;12:744–9.
[31] Dong L, Lou J, Shenoy VB. Large in-plane and vertical piezoelectricity in Janus transition metal dichalchogenides. ACS Nano 2017;11:8242–8.
[32] Li F, Wei W, Zhao P, Huang B, Dai Y. Electronic and optical properties of pristine and vertical and lateral heterostructures of Janus MoSSe and WSSe. J Phys Chem Lett 2017;8:5959–65.
[33] Yin WJ, Wen B, Nie GZ, Wei XL, Liu LM. Tunable dipole and carrier mobility for a few layer Janus MoSSe structure. J Mater Chem C 2018;6:1693–700.
[34] Song WG, Kwon H, Park J, Yeo J, Kim M, Park S, et al. High Performance Flexible Multilayer MoS2 Transistors on Solution Based Polyimide Substrates. Adv Funct Mater 2016;26:2426–34.
[35] Kadantsev ES, Hawrylak P. Electronic Structure of Single MoS2 Monolayer. Solid State Commun 2012;152:909–13.
[36] Kumar A, Ahluwalia P.K. Electronic Structure of Transition Metal Dichalcogenides Monolayers 1H-MoS2 (M = Mo, W, X = S, Se, Te) from ab Initio Theory: New Direct Band Gap Semiconductors. Eur Phys J B 2012; 85: 186.
[37] Kumar A, Ahluwalia PK. A First Principle Comparative Study of Electronic and Optical Properties of 1H-MoS2 and 2H-MoS2. Mater Chem Phys 2012;135:755–61.
[38] Ataca C, Shahin H, Aktruk E, Ciraci S. Mechanical and Electronic Properties of MoS2 Nano Ribbons and Their Defects. J Phys Chem C 2011;115:3934–41.
[39] Fan XF, Chang CH, Zheng WT, Kuo JL, Singh DJ. The electronic properties of single-layer and multilayer MoS2 under high pressure. J Phys Chem C 2015;119:10189–96.
[40] Dou XM, Ding K, Jiang DS, Fan XF, Sun BQ. Probing spin-orbit coupling and interlayer coupling in atomically thin molybdenum disulfide using hydrostatic pressure. ACS Nano 2016;10:1619–24.
[41] Perdew JP, Burke K, Ernzerhof M. Generalized gradient approximation made simple. Phys Rev Lett 1996;77:3865–8.
[42] Kresse G, Furthmüller J. Efficient iterative schemes for ab initio total-energy calculations using a plane-wave basis set. Phys Rev B 1996;54:11169–83.
[43] Blöchl PE. Projector augmented-wave method. Phys Rev B 1994;50:17953–79.
[44] Klimeš J, Bowler DR, Michaelides A. Chemical accuracy for the van der Waals density functional. J Phys Condens Mat 2009;22:022201.
[45] Monkhorst HJ, Pack JD. Special points for Brillouin-zone integrations. Phys Rev B 1976;13:5188–92.
[46] Jung C, Kim S. M, Moon H, Han G, Kwon J, Hong Y.K, Omkaram I, Yoon Y, Kim S, Park J. Highly Crystalline CVD-grown Multilayer MoSe2 Thin Film Transistor for Fast Photodetector. Sci. Rep. 2015; 5: No. 15313.
[47] Gao W, Wang M, Ran C, Li L. Facile one-pot synthesis of MoS_2 quantum dots–graphene–TiO_2 composites for highly enhanced photocatalytic properties. Chem Commun 2015;51:1709–12.
[48] Lehtinen O, et al. Atomic Scale Microstructure and Properties of Se-Deficient Two-Dimensional $MoSe_2$. ACS Nano 2015;9:3274–83.
[49] Li H, et al. Activating and optimizing MoS_2 basal planes for hydrogen evolution through the formation of strained sulphur vacancies. Nat Mater 2016;15:48–53.
[50] Xi T, Zengxi W, Quanhui L, Jianmin Ma. Strain engineering the D-band center for Janus MoSSe edge: Nitrogen fixation. J Energy Chem 2019;33:155–9.
[51] Jian-Dong L, Zeng-Xi W, Yu-Hai D, Yue-Zhan F, Jian-Min Ma. Ru-doped phosphorene for electrochemical ammonia synthesis. Rare Met 2020;39:874–80.